Hindawi
Journal of Robotics
Volume 2023, Article ID 4820479, 10 pages
https://doi.org/10.1155/2023/4820479

*Research Article*

# Adaptive Control Algorithm for Trajectory Tracking of Underactuated Unmanned Surface Vehicle (UUSV)

**Chandanlal Karnani [1,2] Syed Akhter Raza,[1] Muhammad Asif [3] and Muhammad Ilyas[4]**

[1]*Department of Computer Science, Federal Urdu University of Arts, Science and Technology, Karachi, Pakistan*
[2]*Department of Computer Science & IT, Sir Syed University of Engineering & Technology, Karachi, Pakistan*
[3]*Faculty of Engineering, Science, Technology & Management, Ziauddin University, Karachi, Pakistan*
[4]*Government College University, Hyderabad, Pakistan*

Correspondence should be addressed to Chandanlal Karnani; chandan.lal@fuuast.edu.pk

Received 19 October 2022; Revised 17 January 2023; Accepted 3 February 2023; Published 17 February 2023

Academic Editor: Ting Zou



The ability to track the trajectory or path on the sea surface remains a key measurement in the control system of an unmanned surface vehicle (USV). In this research, the designed algorithm defines the path and minimizes the disturbances to zero. Underactuated USVs are ships or boats, which operate on the water surface without a crew and the underactuated system has low actuators than its degree of freedom (DOF). The adaptive control strategy is applied to the unbounded system as the ocean due to its high performance, while the robust control system attains high performance in the bounded system. To consider the trajectory tracking of UUSV and provide an optimal control strategy for a ship in the presence of external disturbances, the study presents a controller-based on model reference adaptive control with an integrator (MRACI), which guarantees the stability of a closed-loop system. The vehicle experiences variations in the system response due to external disturbance. This abovementioned scheme reduces the variations to nearly equal to zero making the vehicle stable. First, use computer-based simulation to verify the proposed controller under two different scenarios. Then, simulation results show that the designed scheme lowers the errors and performs well.

## 1. Introduction

In recent years, unmanned surface vehicles (USVs) have become more attractive and caught the attention of many researchers all over the world [1]. It attains massive potential to the environment, which includes security, water surveys, monitoring, and military. These vehicles are purposed in marine environments for dull, dirty, and hazardous tasks [2, 3]. This technology provides many qualities which include new vehicle designs and concepts for different missions. Generally, surface vehicles are characteristically fast, smaller in size, and highly maneuverable [4]. In a few years, path planning and trajectory tracking become great attention for the control community. The capability of tracking the path is an essential measurement in the control system [5]. The motivation for this research is to design a control scheme for a surface vehicle that completes the given task effectively. Practically, the disturbance is the basic threat from the environment [6]. This study designs the adaptive control algorithm for trajectory tracking and path planning.

In [7], the study investigates the trajectory tracking problem for surface vehicles. This study presents a novel adaptive fuzzy controller to guarantee the stability of a closed-loop system. The tracking errors can be reduced to small neighborhoods within a fixed time interval. The simulation results verify and demonstrate the validity of the designed control strategy. In [8], the article proposes a sliding mode control scheme for USV using the dynamic system, neural network, backstepping, and sliding mode control. The neural network helps in approximating the system's dynamic uncertainty, which uses single parameters. The tangent function reduces the variations due to the sliding mode surface. Additionally, a neural shunting model helps in reducing and eliminating the problem caused by the backstepping method. The stability of the system is verified by the Lyapunov stability theory. The simulation results validate the effectiveness of the proposed control scheme. Furthermore, in [9], the paper proposes a trajectory tracking controller for USV with input constraints and multiple uncertainties. It also introduces the nonlinear tracking differentiators, which help in attaining a fast-tracking response. For surge and yaw angles, a new guidance law is constructed. The controller design process is modest with guidance law. The simulation results show the stabilization of tracking errors and verify the accuracy and effectiveness of the proposed algorithm. Finally, in [10], the article presents an adaptive trajectory tracking controller for USV. The controller solves the strong coupling problem of control inputs. Furthermore, a guidance trajectory avoids input saturation. The Lyapunov stability helps in attaining bounded stability. Finally, the computational simulations are compared with different methods and verify the accuracy and effectiveness of the proposed scheme.

The main contributions of this research article are as follows.

(I) To design an adaptive control technique for USV that helps in adapting disturbances

(II) To perform the objective of trajectory tracking without or with disturbance in an environment

(III) To show the higher and optimal performance and stability of the system during trajectory tracking

(IV) To add an integrator with the controller in the feedback loop, which rises the order of the system but helps in reducing the errors of the system

This manuscript is organized as follows. Section 1 defines the introduction. The problem statement and the proposed solution are defined in Section 2. Section 3 defines state of the art. Similarly, Sections 4 and 5 define the mathematical model of ship and controller design, respectively. Computational simulations are performed in Section 6. Lastly, Section 7 defines the conclusion of the manuscript.

## 2. Problem Statement and Proposed Solution

This section defines the problem statement and the solution applied to solve the following issue. The main problems are as follows:

(i) Stabilization: The aim is to stabilize [11] the USV by reducing the position and orientation error to zero with respect to the pointed position in an anticipated orientation

(ii) Trajectory tracking: The vehicle requires to track time-parameterized references [12, 13]. This problem can be solved by using nonlinear control laws

This section divides the problem into two different scenarios. In scenario 1, the USV follows the path using the designed controller without disturbance. In scenario 2, trajectory tracking takes place with disturbances using the designed controller. Below, each scenario is described in detail.

*2.1. Scenario 1.* Figure 1 represents the first scenario. In this case, USV starts to track the desired trajectory from the starting position. The environment is free of all the disturbances like wind disturbance. The aim is to complete the trajectory tracking successfully on the reference path while holding the maximum stability in the system.

*2.2. Scenario 2.* Figure 2 represents the second scenario. In this case, USV again starts to track the desired trajectory from the starting position. The environment is not free from disturbances and causes variations and noises in the system response. In this case, it is not easy to follow the track because it interrupts the stability of the system. The aim is to complete the trajectory tracking successfully under the designed scheme on the reference path while holding as maximum stability as possible.

This study presents a USV intending to track the path, i.e., trajectory tracking with or without disturbances in the environment. To attain this, the vehicle reaches to initial position and tries to track the path, but it is difficult in a disturbed environment to track a path because it affects its stabilization and many other factors. To solve these issues, this study presents a model reference adaptive controller with an integrator. This scheme guarantees the stability of a closed-loop system. The system response experiences variations due to disturbance, but this designed scheme reduces the variation nearly to zero.

## 3. State of the Art

This section defines the current trends in this field. In [14], the article presents the positioning system based on stereo vision. This study also proposed an object detection model based on learning to solve the robust detection challenge in a complex environment. Furthermore, two methods, namely, stereo vision and monocular are examined for comparison. The USV is equipped with a positioning system oppressed to verify the accuracy of the system. Computational results show that the designed scheme attains a higher accuracy with a good performance in all scenarios. In [15], the study proposes a method based on optimal control to obtain an optimal path for USV. This method is also called the global path planning method and cannot be applied to complex scenarios. This article defines the obstacle-based modeling approach with path planning problems considering kinematics. The proposed method is then compared with traditional methods under two different scenarios. The simulation results show that the designed scheme is superior in terms of convergence speed and path quality. Similarly, in [16], the article proposes path planning of USVs to rescue the target points in the complex environment of the ocean. The objective is to rescue all targets and turn them back safely to priority points. The contributions of this study are that it proposes a K-means division algorithm to identify the ocean's complex environment and a path planning method to optimize the angular energy. The simulation results with state-of-the-art methods demonstrate that the proposed scheme is superior in terms of collision avoidance and

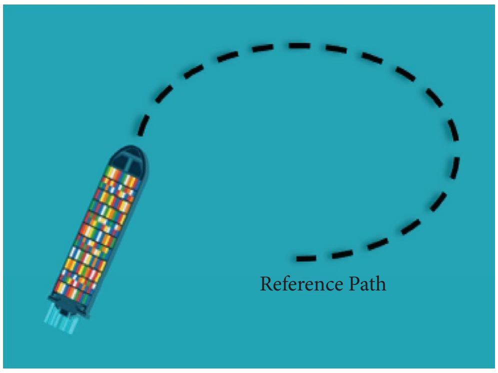


Figure 1: First scenario illustration.

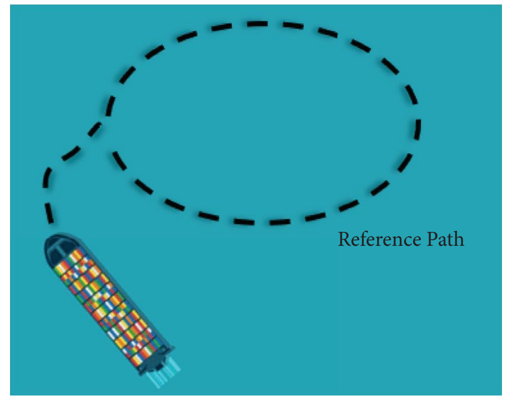


Figure 2: Second scenario illustration.

assignment of the target. In [17], the study designed the sliding mode control (SMC) method for the formation regulation of USVs with environmental disturbances. The formation based on a sliding surface is a troupe in asymptotic stability analysis to reduce the order of the sliding mode system. This study also derived a formation reference function with initial conditions.

## 4. Mathematical Model

This section briefly defines the motion of the marine vehicle, which is divided into two sections kinematics and dynamics.

*4.1. Kinematics.* The geometric motion effects are dealt with in this section. The marine vehicle attains six degrees of freedom (DOF) [18] in 3D. The six variables define their position and orientation, as in Table 1 below.

The position, orientation, linear, and angular velocity of the vehicle are defined as follows:

$$\zeta = \begin{bmatrix} x & y & z & \varphi & \theta & \psi \end{bmatrix}^T, \tag{1}$$

$$v = \begin{bmatrix} u & v & w & p & q & r \end{bmatrix}^T. \tag{2}$$

The two coordinate systems are required to attain the model of a marine vehicle, namely: (1) the Earth coordinate system [19] (ECS) and (2) the body coordinate system [20] (BCS). ECS is used in day-to-day life routines. In this coordinate system, the $x$-axis points toward the north direction, the $y$-axis points toward the east direction, and the $z$-axis point perpendicular to the Earth's surface. Assume that this system is inertial because the marine vehicle has virtually fixed longitude and latitude. So, Newton's laws are applicable. BCS is attached to the marine vehicle used in measuring the linear and angular velocities of the designed system. In this coordinate system, the $x$-axis points to the length of the vehicle from center to front, and the $y$-axis points toward the right side. Figure 3 below clearly defines the concept of both coordinate systems.

The ship or vehicle velocity is transformed from body to Earth frame using the transformation matrix $l$ and equation (1).

$$\dot{\zeta} = lv, \tag{3}$$

whereas

$$l = \begin{bmatrix} \mathcal{R} & O_3 \\ O_3 & \mathrm{T} \end{bmatrix},$$
$$\mathrm{T} = \begin{bmatrix} 1 & s\varphi t\theta & c\varphi t\theta \\ 0 & c\varphi & -s\varphi \\ 0 & \dfrac{s\varphi}{c\theta} & \dfrac{c\varphi}{c\theta} \end{bmatrix}, \tag{4}$$

where a rotation matrix is denoted by $\mathcal{R}$, a square matrix is denoted by $O_3$ having three dimensions, and $s = sin|c = \cos|t = tan$. The matrix $\mathcal{R}$ is considered a component of an orthogonal group of third order and is well-defined as follows:

$$\mathbb{S}\mathrm{O}(3) = \left\{\mathcal{R}|\mathcal{R}\epsilon\mathbb{R}^{3\times 3},\ \mathcal{R}\mathcal{R}^{\mathrm{T}} = \mathcal{R}^{\mathrm{T}}\mathcal{R} = I,\ |\mathcal{R}| = 1\right\}. \tag{5}$$

The Euler angle transformation method is used to calculate the matrix $\mathcal{R}$. It can be represented as

$$\mathcal{R} = \begin{bmatrix} c\psi c\theta & -s\psi c\varphi + c\varphi s\theta s\varphi & s\psi s\varphi + c\psi c\varphi s\theta \\ s\psi c\theta & c\psi c\varphi + s\varphi s\theta s\psi & -c\psi s\varphi + s\theta s\psi c\varphi \\ -s\theta & c\theta s\varphi & c\theta c\varphi \end{bmatrix}. \tag{6}$$

The following lemmas and statements are considered while designing the control system of the vehicle.

**Lemma 1.** *The matrix $\mathcal{R}$ can be written as*

$$\dot{\mathcal{R}} = \mathcal{R}\mathbb{S}(p, q, r), \tag{7}$$

*where as*

$$\mathbb{S}(p, q, r) = \begin{bmatrix} 0 & -r & q \\ r & 0 & -p \\ -q & p & 0 \end{bmatrix}. \tag{8}$$

Table 1: Notations for marine vehicle.

| DOF | Motion | Force moment | Velocity | Movement angle |
|---|---|---|---|---|
| I | In the $x$-direction-surge | $X$ | $u$ | $X$ |
| II | In the $y$-direction sway | $Y$ | $v$ | $Y$ |
| III | In the $z$-direction heave | $Z$ | $w$ | $Z$ |
| IV | About the $x$-axis roll | $K$ | $p$ | $\Phi$ |
| V | About the $y$-axis pitch | $M$ | $q$ | $\Theta$ |
| VI | About the $z$-axis yaw | $N$ | $r$ | $\Psi$ |

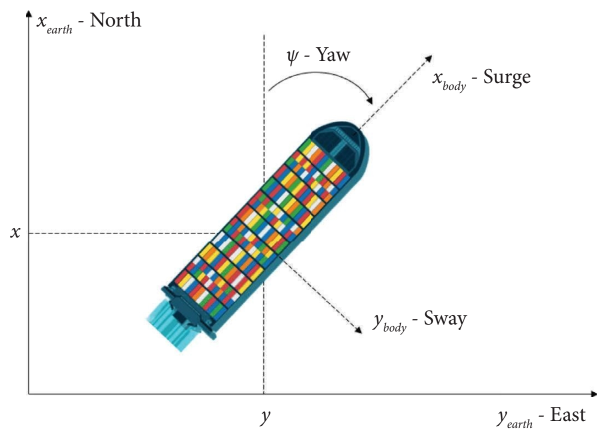


Figure 3: Earth and body frame with heading and position.

**Lemma 2.** *The solution is bounded uniformly if there is a positive and continuous Lyapunov function denoted by $\Gamma(x)$, which satisfies the condition $\alpha_1(x) \leq \Gamma(x) \leq \alpha_2(x)$ such that $\dot{\Gamma}(x) \leq -\rho\Gamma(x) + F$. However, $\alpha_1$ and $\alpha_2$ are functions of class k, the positive constants are $\rho$ and $F$.*

*Statement 1.* The marine vehicle center of gravity (COG) will be located at nonzero $x_g$ and $y_g = 0$ if the vehicle is symmetric on $xz$ plane.

*Statement 2.* The dissimilarity of disturbance is denoted by $e$ and stays bounded and restricted. Thus,

$$\dot{e} \leq \nabla, \tag{9}$$

where $\nabla$ is the constant. The essentials of roll, pitch, and heave will be abandoned for simplification while using surface ships and vehicles. This is done because in these directions, the motion/rotations are identically small. Thus, equation (3) can be written in a simplified form as follows:

$$\dot{\zeta} = \mathcal{R}(\psi)v. \tag{10}$$

Now, $\zeta = \begin{bmatrix} x & y & \psi \end{bmatrix}^T$ and $v = \begin{bmatrix} u & v & r \end{bmatrix}^T$. Furthermore, $\mathcal{R}(\psi)$ can be written as

$$\mathcal{R}(\psi) = \begin{bmatrix} c\psi & -s\psi & 0 \\ s\psi & c\psi & 0 \\ 0 & 0 & 1 \end{bmatrix}. \tag{11}$$

Equation (8) can be rewritten as

$$\mathbb{S}(r) = \begin{bmatrix} 0 & -r & 0 \\ r & 0 & 0 \\ 0 & 0 & 0 \end{bmatrix}. \tag{12}$$

*4.2. Dynamics.* This section deals with the study of forces that helps in causing motion. The equation of dynamics of motion can be written by considering hydrodynamic forces, moments, and statement 1 as follows:

$$m\dot{v} + c(v)v + \partial(v)v = j, \tag{13}$$

where as

$$\begin{aligned} m &= \begin{bmatrix} \eta - X_{\dot{u}} & 0 & 0 \\ 0 & \eta - Y_{\dot{v}} & \eta x_g - Y_{\dot{r}} \\ 0 & \eta x_g - Y_{\dot{r}} & I_z - N_{\dot{r}} \end{bmatrix}, \\ c(v) &= \begin{bmatrix} 0 & 0 & c_{23}(v) \\ 0 & 0 & -c_{23}(v) \\ -c_{13}(v) & c_{23}(v) & 0 \end{bmatrix}, \\ \partial(v) &= -\begin{bmatrix} -X_u + X_{u|u|}|u| + X_{uuu}u^2 & 0 & 0 \\ 0 & -Y_v + Y_{v|v}|v| + Y_{|r|v}|r| & -Y_r + Y_{|v|r}|v| + Y_{|r|r}|r| \\ 0 & -N_v + N_{v|v}|v| + N_{|r|v}|r| & -N_r + N_{|v|r}|v| + N_{|r|r}|r| \end{bmatrix}, \end{aligned} \tag{14}$$

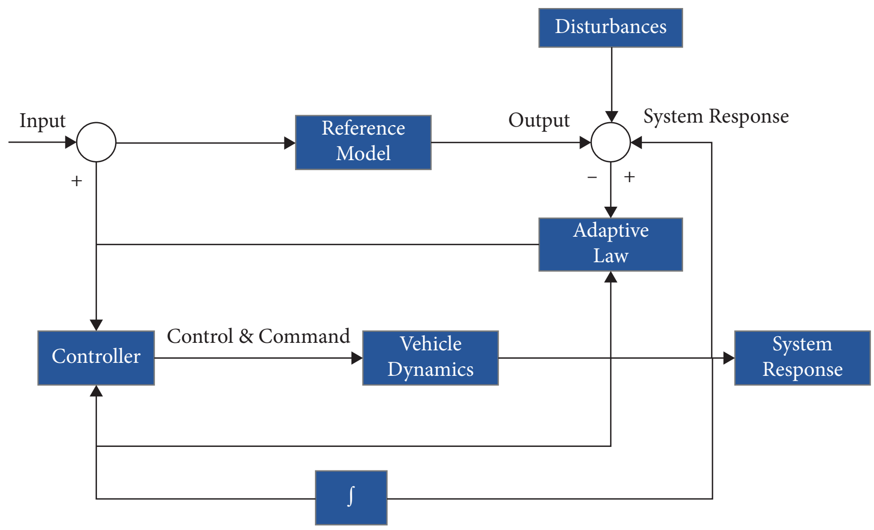


Figure 4: Control structure of the controller with integral feedback.

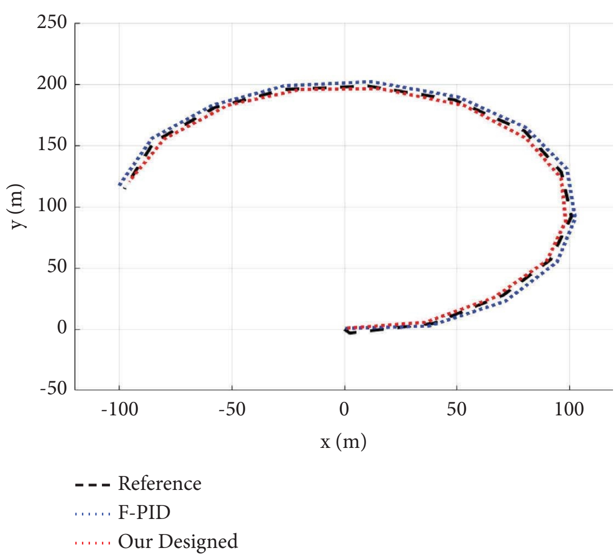


Figure 5: Trajectory tracking of USV.

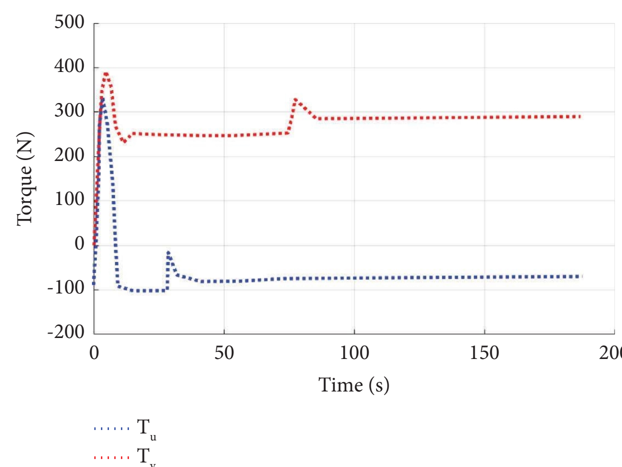


Figure 6: Torque curves with respect to time.

where the mass of the ship is denoted by $\eta$, and the inertia of the moment along the $z$-axis is represented by $I_z$. The hydrodynamic parameters are ($N_{\cdot}$, $X_{\cdot}$, and $Y_{\cdot}$), $c_{13}(v) = Y_{\dot{v}}(v) + Y_{\dot{r}}(r) - \eta(v + x_g r)$, and $c_{23}(v) = X_{\dot{u}}(u) - \eta u$. The overall mathematical model of the vehicle can be written as follows:

$$\begin{cases} \dot{\zeta} = Rv, \\ m\dot{v} + c(v)v + \partial(v)v = j + \lambda, \end{cases} \tag{15}$$

where the peripheral disturbance in the system is denoted by $\lambda$.

## 5. Controller Designing

In the last few years, different types of adaptive controllers had been used for both linear and nonlinear systems. But when it comes to the dynamics controling of an autonomous vehicle, a model reference adaptive controller (MRAC) is the optimal solution. As shown in Figure 4, it attains the reference model and adaptive law, which is defined as the response of the system. Similarly, disturbances are added, for example, wind disturbance to offset the uncertainties. If the response of the system is differing, the adaptive law changes the output. According to the demand of the controller, the vehicle tunes its dynamics. The steady-state errors are diminished by the integral [21].

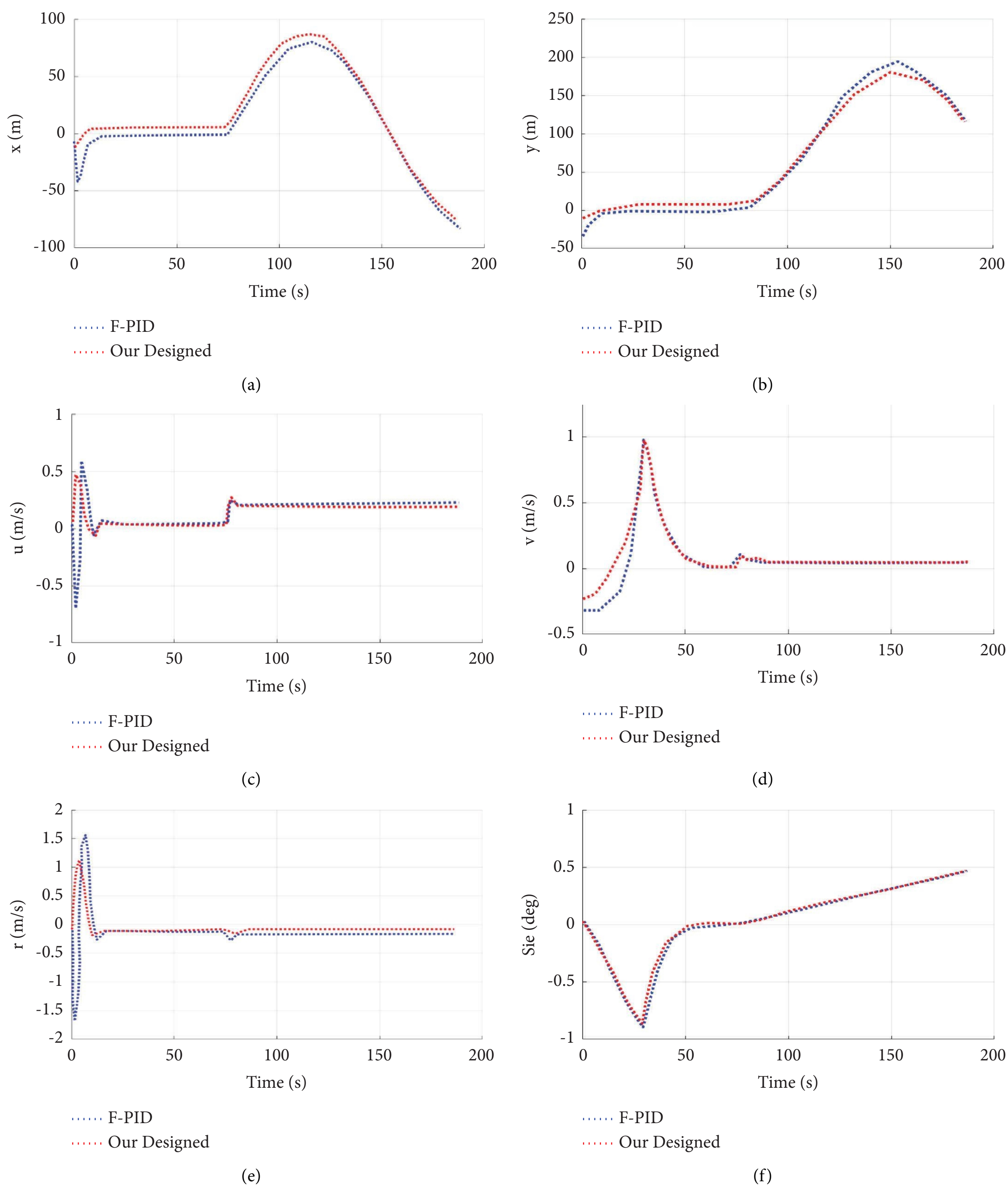


FIGURE 7: (a–f) state curves of USV with respect to time.

The uncertainties guarantee the dynamics of the system as well as identical conditions, which are as follows:

$$\left\{ \dot{R}_K(t) = X_K(t)R_K(t) + (u)(t) + M\left(R_K(t)\right) + Y_K(t) + T, S_K(t) = Z_K(t)R_K(t), \right. \tag{16}$$

where $R_K(t)$ defines the vehicle time-dependent state variables, and $S_K(t)$ defines the time-dependent output.

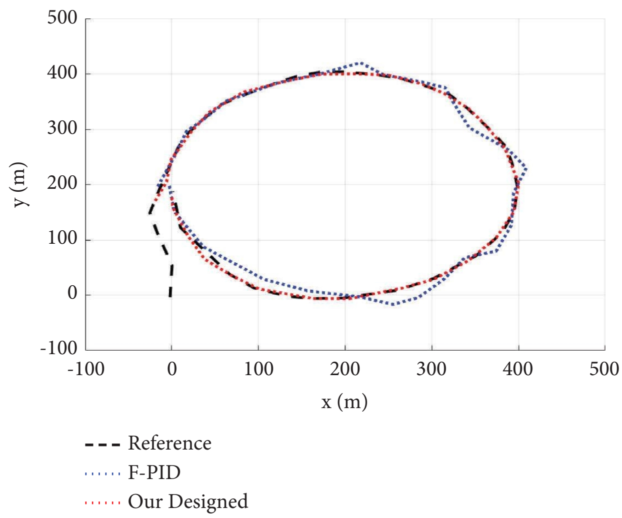


Figure 8: Trajectory tracking of USV.

The matrices of the vehicle are $X_K(t)$, $Y_K(t)$, and $Z_K(t)$. The nonlinear function of $R_K(t)$ is $M$. The total torque is defined as $T = T_{\text{input}} + T_{\text{extenal}}$.

$$M(R_K(t)) = \gamma_a^{\tau}\sigma_a(R_K(t)), \tag{17}$$

where $\gamma_a^{\tau}$ denotes the parametric matrix, and Lipchitz vector is denoted by $\sigma_a$. The multiple input and multiple output assumptions are taken as follows:

$$\begin{cases} \dot{R}_K(t) = X_K(t)R_K(t) + Y_K(t)M(R_K(t)), \\ S_K(t) = Z_K(t)R_K(t). \end{cases} \tag{18}$$

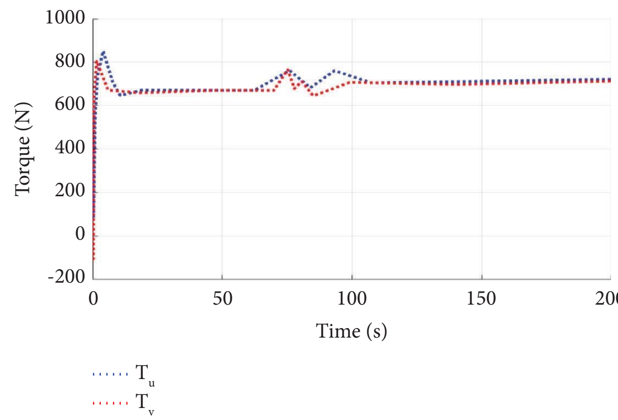


Figure 9: Torque curves with respect to time.

The tracking error is given as follows:

$$E_{S_K(t)=}S_K(t) - S_p(t). \tag{19}$$

The integrated tracking error of output is attained as follows:

$$\dot{E}_{S_I} = E_S(t) = S_K(t) + S_p(t), \tag{20}$$

where the output tracking error is denoted by $E_S(t)$. The open-loop vehicle dynamics are given as follows:

$$\overbrace{\begin{pmatrix} \dot{h}_{S_I}(t) \\ \dot{R}_K(t) \end{pmatrix}}^{\dot{h}} = \overbrace{\begin{pmatrix} O_{m\times m} & Z_K(t) \\ O_{n_K\times m} & X_K(t) \end{pmatrix}}^{X} + \overbrace{\begin{pmatrix} E_{S_I}(t) \\ R_K(t) \end{pmatrix}}^{R} + \overbrace{\begin{pmatrix} O_{m\times m} \\ Y_K(t) \end{pmatrix}}^{Y} \times \overbrace{(u(t) + \gamma_a^{\tau}\sigma_a(R_K(t)))}^{aR_K(t)} + \overbrace{\begin{pmatrix} -I_{m\times m} \\ O_{n_K\times m} \end{pmatrix}}^{Y_p(t)} S_p(t)S(t) = \overbrace{O_{m\times m}Z_K(t)R(t)}^{Z(t)}. \tag{21}$$

The control input of the open loop is denoted by $u(t)$ and the output is denoted by $S(t)$. The improved tracking error is defined as $\dot{E}_{S_I} = Z_K(t)R_K(t) - S_K(t)$. The known constant matrix is denoted by $Z_K(t)$. The order of the system is $n = n_K + m$. The parametric uncertainty is defined as $\gamma_a^{\tau}\sigma_a(R_K(t)$. The regressor vector is dented by $\sigma_a(R_K(t)$. From a restricted locality origin, there would be a finite constant, and inequity is defined as follows:

$$\begin{aligned} &0 < Q_{\sigma_a}, && (R_1(t), R_2(t)\epsilon R^{n_K}, \\ &\sigma_a(R_1) - \sigma_a(R_1(t), R_2(t)\epsilon R^{n_K} \leq Q_{\sigma_a}, && R_1(t) - R_2(t). \end{aligned} \tag{22}$$

*Assumption 1.* In the ostensible system, the pair of matrices $(X_K(t), Y_K(t))$ is governable and under control. The matrix's controllability is linked with the condition of rank given as follows:

$$\text{rank}\begin{pmatrix} X_K(t) & Y_K(t) \\ Z_K(t) & 0_{K\times L} \end{pmatrix} = n_K + L = W. \tag{23}$$

Neglecting the system uncertainties, the standard reference model is given as follows:

$$\dot{R}_p(t) = X_p(t)R_p(t) + Y_p(t)S_p(t), \tag{24}$$

whereas

$$X_p(t) = X(t) - Y(t)\left(U_p^{-1}Y_K^{\tau}(t)V_p\right). \tag{25}$$

The feedback gain of the linear quadratic regulator (LQR) is denoted by $(U_p^{-1}Y_K^{\tau}(t)V_p)$. The positive exact solution of $V_p$ is given as follows:

$$V_pX(t) + X^{\tau}(t)V_p - V_pY(t)U_p^{-1}Y^{\tau}(t)V_p + D_p = 0, \tag{26}$$

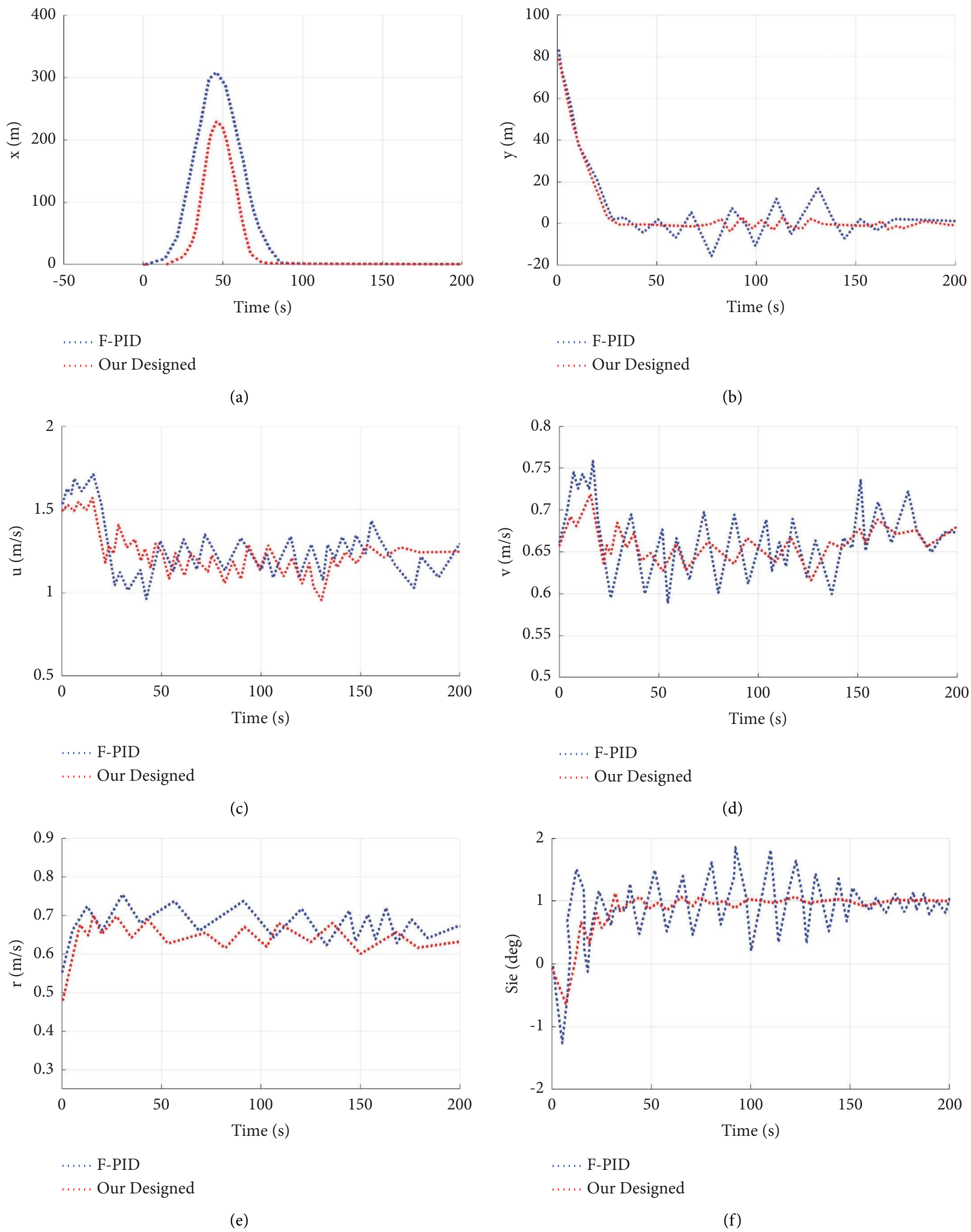


Figure 10: (a–f) state curves of USV with respect to time.

where the symmetric positive matrices are denoted by $V_p, D_p$.

*Assumption 2.* Consider a diagonal matrix $d$ and matrix $X_p(t)$. The gain matrix $H_R$ is given as follows:

$$X_p(t) = X(t) - Y(t) d H_R^{\tau}. \tag{27}$$

For controllable matrix $(X_K(t), Y_K(t))$ and nonsingular matrix $d$, $H_R$ is assured. Eliminate $X(t)$, $Y(t)$, and take the inverse of $d$ by relating equations (25) and (27) resulting in the following:

$$H_R = d^{-1}\left(U_p^{-1} Y_K^{\tau}(t) V_p\right). \tag{28}$$

The dynamics of the vehicle are rewritten in the following equation (27)

$$\dot{X}(t) = X_p(t)X(t) + Y(t)d(u(t)) + \left[H_R^{\tau}X(t) + \gamma_a^{\tau}\sigma_a\left(R_K(t)\right) + Y_U(t)S_p(t)\right]. \tag{29}$$

Finally,

$$\dot{X}(t) = X_p(t)X(t) + Y(t)d(u(t)) + \left[\gamma_a^{\tau}\sigma_a\left(R_K(t)\right) + Y_U(t)S_p(t)\right]. \tag{30}$$

## 6. Simulation Results

This section presents the simulations, which verify the accuracy and effectiveness of the designed control algorithm in two different scenarios, i.e., without and with disturbance. MATLAB software is used for the simulation results. The initial position of the vehicle is $(0, 0)$ with an engine speed of 40RPM and a vehicle speed of 11knots. The speed of wind is approximately $8\,m/s$ with the direction of $90^{\circ}$. This section provides the comparison of the designed scheme with fuzzy-PID in two different scenarios, as mentioned above. The speed and heading of the vehicle can be changed at any time. Thus, the relationship between the disturbance and the vehicle also changes.

*6.1. Scenario 1.* In this case, the simulation results show the trajectory tracking of USV with two controllers (F-PID and designed scheme) without disturbance. The main objective, in this case, is to follow the path and reach the targeted position safely.

Figure 5 shows the trajectory tracking of vehicles under the designed scheme. It is seen from Figure 5 that the USV arrives at its starting position, tracks the path well nearly to the reference path with the designed scheme, and reaches the targeted position. Figure 6 shows the USV variation curves of torque in terms of $T_u$ and $T_v$ with respect to time. Figures 7(a)–7(f) show the control inputs and state curves of USV. It is observed that the USV positions to the expected value in 15 seconds, and then the orientation converges to the expected value within 80 seconds.

*6.2. Scenario 2.* In this case, the simulation results show the trajectory tracking of USV with two controllers (F-PID and designed scheme) with disturbance. The main objective, in this case, is to follow the path and reach the targeted position safely by avoiding disturbances.

Figure 8 shows the trajectory tracking of vehicles under the designed scheme. It is seen from Figure 8 that the USV arrives at its starting position, tracks the path well nearly to the reference path with the designed scheme, and reaches the targeted position by reducing the effects of disturbances. Figure 9 shows the USV variation curves of torque in terms of $T_u$ and $T_v$ with respect to time. Figures 10(a)–10(f) show the control inputs and state curves of USV. It is observed that the USV positions to the expected value in 20 seconds, and then the orientation converges to the expected value within 70 seconds. As seen in Figure 10, the performance of the designed scheme is quite effective as compared to another controller. It reduces the oscillations and performs well.

## 7. Conclusion

This paper addresses the trajectory tracking of unmanned surface vehicles (USVs). Specifically, it also presents the mathematical model of the ship in terms of kinematics and kinetics. It also designs the model reference adaptive controller with an integrator (MRACI). Due to external disturbances, the vehicle experiences some fluctuations and variations in the system response. The designed control strategy reduces these errors and makes the vehicle as much as possible. The Simulink (MATLAB) is used to simulate the designed scheme with and without disturbance. The simulation results verify the effectiveness of the controller and guarantee stability in the system.

## Data Availability

The data supporting the current study are given in the article.

## Conflicts of Interest

The authors declare that they have no conflicts of interest.

## References


[1] J. Xin, J. Zhong, S. Li, J. Sheng, and Y. Cui, “Greedy mechanism-based particle swarm optimization for path planning problem of an unmanned surface vehicle,” *Sensors*, vol. 19, pp. 4620–21, 2019.

[2] L. Kunze, N. Hawes, T. Duckett, M. Hanheide, and T. Krajník, “Artificial intelligence for long-term robot autonomy: a survey,” *IEEE Robotics and Automation Letters*, vol. 3, no. 4, pp. 4023–4030, 2018.

[3] R. P. Pedrozo, “US employment of marine unmanned vehicles in the South China Sea,” in *The South China Sea*, pp. 217–229, Routledge, New York, NY, USA, 2019.

[4] E. Begovic, “Advance speed-hull-pump-jet interactions in small ASV,” in *HSMV 2020: Proceedings of the 12th*

*Symposium on High-Speed Marine Vehicles*vol. 5, p. 197, IOS Press, Washington, DC, USA, 2020.

[5] X. Yan, D. Jiang, R. Miao, and Y. Li, “Formation control and obstacle avoidance algorithm of a multi-USV system based on virtual structure and artificial potential field,” *Journal of Marine Science and Engineering*, vol. 9, no. 2, p. 161, 2021.

[6] I. Linkov and A. Kott, “Fundamental concepts of cyber resilience: introduction and overview,” *Cyber Resilience of Systems and Networks*, pp. 1–25, Springer, New York, NY, USA, 2019.

[7] S. Song, Ju H. Park, B. Zhang, and X. Song, “Event-triggered adaptive practical fixed-time trajectory tracking control for unmanned surface vehicle,” *IEEE Transactions on Circuits and Systems II: Express Briefs*, vol. 68, no. 1, pp. 436–440, 2021.

[8] B. Qiu, G. Wang, Y. Fan, D. Mu, and X. Sun, “Adaptive sliding mode trajectory tracking control for unmanned surface vehicle with modeling uncertainties and input saturation,” *Applied Sciences*, vol. 9, no. 6, p. 1240, 2019.

[9] H. Huang, M. Gong, Y. Zhuang, S. Sharma, and D. Xu, “A new guidance law for trajectory tracking of an underactuated unmanned surface vehicle with parameter perturbations,” *Ocean Engineering*, vol. 175, pp. 217–222, 2019.

[10] X. Sun, G. Wang, and Y. Fan, “Adaptive trajectory tracking control of vector propulsion unmanned surface vehicle with disturbances and input saturation,” *Nonlinear Dynamics*, vol. 106, no. 3, pp. 2277–2291, 2021.

[11] G. Guo and P. Zhang, “Asymptotic stabilization of USVs with actuator dead-zones and yaw constraints based on fixed-time disturbance observer,” *IEEE Transactions on Vehicular Technology*, vol. 69, no. 1, pp. 302–316, 2020.

[12] Y. Zhao, X. Qi, Y. Ma, Z. Li, R. Malekian, and M. A. Sotelo, “Path following optimization for an underactuated USV using smoothly-convergent deep reinforcement learning,” *IEEE Transactions on Intelligent Transportation Systems*, vol. 22, no. 10, pp. 6208–6220, 2021.

[13] Q.. Yao, “Fixed-time trajectory tracking control for unmanned surface vessels in the presence of model uncertainties and external disturbances,” *International Journal of Control*, vol. 95, no. 5, pp. 1133–1143, 2022.

[14] Ø. Volden, A. Stahl, and T. I. Fossen, “Vision-based positioning system for auto-docking of unmanned surface vehicles (USVs),” *International Journal of Intelligent Robotics and Applications*, vol. 6, no. 1, pp. 86–103, 2022.

[15] D. Ma, S. Hao, W. Ma, H. Zheng, and X. Xu, “An optimal control-based path planning method for unmanned surface vehicles in complex environments,” *Ocean Engineering*, vol. 245, Article ID 110532, 2022.

[16] X. Jin and M. J. Er, “Cooperative path planning with priority target assignment and collision avoidance guidance for rescue unmanned surface vehicles in a complex ocean environment,” *Advanced Engineering Informatics*, vol. 52, Article ID 101517, 2022.

[17] X. Jiang and G. Xia, “Sliding mode formation control of leaderless unmanned surface vehicles with environmental disturbances,” *Ocean Engineering*, vol. 244, Article ID 110301, 2022.

[18] Q. Meng, X. Lai, Ze Yan, Y. Wang, and M. Wu, “Position control with zero residual vibration for two degrees-of-freedom flexible systems based on motion trajectory optimization,” *Information Sciences*, vol. 575, no. 2021, pp. 698–713, 2021.

[19] A. O. Andreev, Yu A. Nefedyev, N. Y. Demina, L. A. Nefediev, N. K. Petrova, and A. A. Zagidullin, “Development of methods for navigational referencing of circumlunar spacecrafts to the selenocentric dynamic coordinate system,” *Astronomy Reports*, vol. 64, no. 9, pp. 795–803, 2020.

[20] K. Heo and Y.-R. Choi, “Investigation on the generalized hydrodynamic force and response of a flexible body at different reference coordinate system,” *Journal of the Society of Naval Architects of Korea*, vol. 58, no. 6, pp. 348–357, 2021.

[21] R. J. Masood, D.Bo Wang, Z. Anwar Ali, and M. Anwar, “Adaptive hybrid control scheme for controlling the position of coaxial tri-rotor UAS,” *Intelligent Automation & Soft Computing*, vol. 25, no. 2, 2019.